

LETTERS

Influencing Strong Field Excitation Dynamics through Molecular Structure

Noel P. Moore, Alexei N. Markevitch, and Robert J. Levis*

*Department of Chemistry, Wayne State University, Detroit, Michigan 48202**Received: August 2, 2001; In Final Form: November 5, 2001*

We report the loss of discrete above-threshold ionization photoelectron peaks in the strong-field (800 nm, 60 fs, $3.6 - 9.0 \times 10^{13} \text{ W}\cdot\text{cm}^{-2}$) excitation in a series of polyatomic molecules of increasing characteristic length. The molecules, biphenyl ($\text{C}_{12}\text{H}_{10}$), diphenylmethane ($\text{C}_{13}\text{H}_{12}$), and diphenylethane ($\text{C}_{14}\text{H}_{14}$), have two phenyl groups spaced by a bridge of zero, one, or two carbon atoms. The photoelectron spectra correlate with the characteristic lengths, not the number of atoms, of these molecules. The molecules having the smallest and largest numbers of atoms (but similar characteristic lengths) display a broad featureless distribution of photoelectron kinetic energies, peaked at lower kinetic energies and extending to many tens of electronvolts. Diphenylmethane, the molecule with intermediate number of atoms but the smallest characteristic length, displays a photoelectron spectrum containing discrete peaks in this range of laser intensities. The absence of discrete photoelectron peaks in the spectra of biphenyl and diphenylethane is interpreted using an eigenstate lifetime model based on calculated field ionization rates in an intense laser field. Finally, the abundance of photoelectrons with high kinetic energies suggests higher probability of electron rescattering in the polyatomic molecules in comparison with atomic intense field ionization.

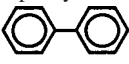
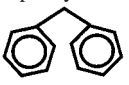
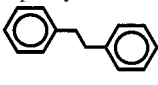
Introduction

The interaction of strong-field radiation with polyatomic molecules is proving to be a rich area for chemical physics. Recent investigations^{1–4} report the effect of molecular size on the coupling and partitioning of intense laser radiation into large polyatomic molecules. Both photoion and photoelectron measurements reveal that coupling from the laser field into a molecule becomes more effective with increasing molecular size. The detailed shape of the photoelectron energy distribution has revealed a systematic correlation with the size of a molecule.¹ In the series of molecules benzene, naphthalene and anthracene, the contribution of discrete peaks arising from above threshold ionization (ATI)⁵ to the total electron yield was observed to decrease with increasing size.³ The maximum kinetic energy and ionization probability also increased with molecular size. These trends suggest that some aspect of molecular size is important in the energy–molecule coupling event. To account

for molecular size, the concept of the *characteristic length* of a molecule has been introduced⁶ as the longest distance within the electrostatic potential energy surface of a molecule, for which the surface does not exceed the first binding energy of the system. Here we test whether the characteristic length can be used to rationalize the photoelectron distributions for three molecules having very similar numbers of atoms but different characteristic lengths.

The specific effect of the characteristic length on strong-field excitation of molecules has been probed using photoelectron spectroscopy. The loss of discrete ATI photoelectron peaks in the series benzene, naphthalene, anthracene³ could be attributed to several mechanisms. One possible explanation is that during strong-field excitation, an electronic eigenstate lifetime mechanism broadens the discrete photoelectron peaks more as the molecular size increases. This model was developed to explain the broadened photoelectron peaks in naphthalene with increas-

TABLE 1: Molecular Properties and Calculated Parameters for Biphenyl, Diphenylmethane, and Diphenylethane

molecule	biphenyl	diphenylmethane	diphenylethane
structure			
formula	C ₁₂ H ₁₀	C ₁₃ H ₁₂	C ₁₄ H ₁₄
molecular weight, amu	154	168	182
characteristic length, a_0 , Å	10.30	7.98	12.52
ionization potential, eV	8.37	8.81	9.1
Δ_0 , nm ^a	280	230	225
$I_{\text{med}} \times 10^{14}$, W cm ⁻²	0.8	5	1.3
WKB transmission probability, w (atomic units), at 2×10^{13} W cm ⁻²	0.0396	0.00166	0.0978
electronic eigenvalue uncertainty, eV at 2×10^{13} W cm ⁻²	1.08	0.045	2.66

^a *UV Atlas of Organic Compounds*; VerlagChemie and Butterworth: Weinheim and London, 1966–1971; Vols. I–V.

ing laser intensity.⁷ This mechanism for the broadening of discrete features involves an increase in the uncertainty of electronic eigenvalues as a consequence of the decrease in lifetime of the electronic states populated during excitation. The decreased lifetime is due to an increased ionization probability at higher laser intensities. Another possibility is an increase in incoherent emission of photoelectrons as the size of a molecule increases. This may be due to the enhanced probability for nonadiabatic multielectron dynamics² (NMED) as the complexity of a molecule increases. The strong incoherent excitation would destroy the interference effects, leading to the ATI features in a modulated emission of the electron kinetic energy distribution.^{8,9} Relative quantitative predictions can be made as a function of laser intensity and molecular parameters for both mechanisms.

The broadening in electronic state energy may be an important factor in the recent spate of intense laser control experiments. Shaped intense laser pulses at 800 nm have been used to control electronic^{10,11} and nuclear^{12,13} wave packet dynamics in closed-loop¹⁴ experiments. To understand the mechanism of such control experiments, we are currently investigating energy coupling in the strong field regime.

Here, we present the photoelectron spectra of biphenyl (C₁₂H₁₀), diphenylmethane (C₁₃H₁₂), and diphenylethane (C₁₄H₁₄). The structures of these molecules are shown in Table 1. Although the molecular size increases marginally and continuously in the series, the characteristic length does not. Due to the shape of these molecules, the molecule of intermediate size, diphenylmethane, has the smallest characteristic length. Thus, with this series, we can delineate whether the loss of discrete photoelectron peaks correlates with molecular size or with characteristic length. The strong-field photoelectron spectra are reported at intensities ranging from 3.6 to 9.0×10^{13} W·cm⁻². The results are interpreted in terms of the structure-based model to determine the extent of lifetime broadening and NMED. We also present evidence for a high probability for electron rescattering in these molecules.

Experimental Section

The electron kinetic energy distributions were recorded using a linear μ -metal shielded time-of-flight photoelectron spectrometer with length of ~ 0.3 m, as described previously.³ Biphenyl and diphenylethane were allowed to sublime directly into vacuum to attain the desired pressure of 1.0×10^{-6} Torr, while diphenylmethane (liquid at room temperature) was admitted effusively into the target chamber. The background pressure of the spectrometer was 1.0×10^{-8} Torr. Samples were excited using a 10 Hz regeneratively amplified laser centered at 800 nm having pulse duration of 60 fs and pulse energy up to 1.5 mJ/pulse, as described previously.⁶ Photoelectron spectra were

measured using laser intensities up to 2.5×10^{14} W·cm⁻². Absolute laser intensities were determined using the laser energy, pulse duration, and focal spot size. The intensities were also calibrated by comparison to the ionization of argon. The laser intensity was attenuated by inserting glass cover slides with known transmission properties into the beam path. No measurable effect on laser pulse duration was introduced by this intensity attenuation.

Results

The photoelectron spectra of biphenyl, diphenylmethane and diphenylethane excited at laser intensities ranging from 3.6 to 9.0×10^{13} W·cm⁻² are presented in Figure 1. Higher laser intensities produced a broad featureless distribution for each molecule similar to Figure 1d. The smallest molecule, biphenyl, and the largest molecule, diphenylethane, yield qualitatively similar photoelectron spectra at all laser intensities employed in this experiment. Above 4.0×10^{13} W·cm⁻², the photoelectron spectra of biphenyl and diphenylethane exhibit similar broad featureless distributions of photoelectron kinetic energies, peaked at lower energies and extending to many tens of electronvolts. The modal kinetic energies for biphenyl and diphenylethane are approximately the same (9.5 ± 1.0 eV) at 6.6×10^{13} W·cm⁻². The maximum kinetic energies for biphenyl and diphenylethane are also similar, extending to 80 eV at 6.6×10^{13} W·cm⁻². At the lowest laser intensity investigated here, 3.6×10^{13} W·cm⁻², the photoelectron spectra of both biphenyl and diphenylethane display weak but discrete photoelectron peaks superimposed on the featureless distribution. These peaks in photoelectron yield are separated by the photon energy, which at 800 nm is 1.55 eV, and represent ATI. Diphenylmethane, which is intermediate in size compared to the other two molecules, displays markedly different photoelectron spectra, with discrete photoelectron peaks visible at all laser intensities investigated. The origin of the ATI features occurs at 0.58 eV, with subsequent ATI peaks spaced by the photon energy, as shown in Figure 1e.

Discussion

The dominant trend in the spectra presented in Figure 1 is that diphenylmethane displays markedly enhanced signal intensities for discrete, well-resolved photoelectron peaks in comparison with biphenyl and diphenylethane over the laser intensity range investigated. To understand the appearance of the strong-field photoelectron spectra for these molecules, we investigate both the lifetime broadening⁷ of the electronic states populated during the excitation and the nonresonant nonadiabatic electronic excitations.²

The lifetime broadening approach relies on employing the ionization rate to provide a limit on the lifetime of a given state. The lower limit of the intense field ionization rate is estimated

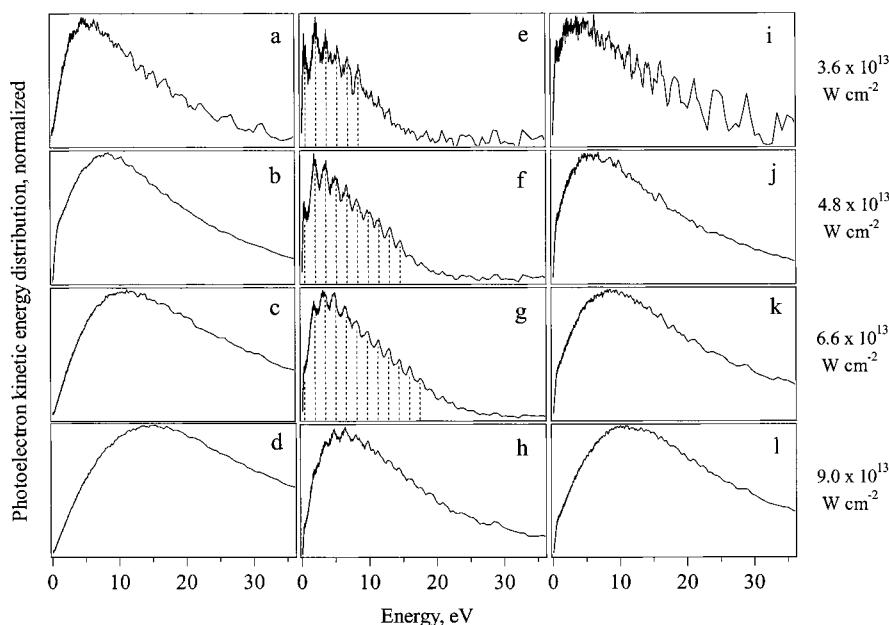


Figure 1. Photoelectron spectra for biphenyl (a, b, c, d), diphenylmethane (e, f, g, h), and diphenylethane (i, j, k, l) excited using 800 nm, 60 fs, of intensity 3.6 , 4.8 , 6.6 and $9.0 \times 10^{13} \text{ W}\cdot\text{cm}^{-2}$, respectively.

using the structure-based tunnel ionization model.¹⁵ At the laser intensities and frequencies employed in this work, several competing mechanisms (such as multiphoton ionization) contribute to the total ionization rate. In principle, any mechanism by which ionization rates increase with laser intensity could induce broadening of the electronic eigenvalues with increasing laser intensity. To explain the results presented here, a mechanism that correlates with molecular structure has been used.

The structure-based calculation estimates spatial delocalization of electrons in molecular orbitals by defining the *characteristic length*: a one-dimensional metric of the molecular wave function. The characteristic length is used as the width of a rectangular well approximating the spatial delocalization of the electrostatic potential of the molecule. Figure 2 shows the characteristic lengths of biphenyl, diphenylmethane, and diphenylethane calculated in a field-free case. To calculate the characteristic length, the electrostatic potential energy surfaces for these molecules were obtained by an ab initio method, by first optimizing the neutral geometry of the species and then calculating the one-dimensional potential energy surfaces along various possible directions. The calculations were performed using the Gaussian¹⁶ electronic structure package at the Hartree–Fock level of theory using the 6-311g* basis set. The one-dimensional potential energy surface having the largest uninterrupted distance between classical turning points at the ionization potential of the molecule specifies the characteristic length. The potential is approximated by a one-dimensional rectangular well, where the height is defined by the ionization potential of the system and the width by the characteristic length. If one superimposes the electric field strength of the laser on the rectangular well, a barrier is formed through which electrons may tunnel ionize. This model then represents a quasi-static representation of the laser-molecule interaction.

It is obvious that at the field intensities employed in this work, both the electrostatic potential energy surface and the electronic eigenstates are significantly perturbed by the laser field.¹⁷ This may have significant implications for determination of the tunnel rates using the structure-based model. In particular, both the ionization potential and the characteristic length may change in the field in comparison with their field-free values. The

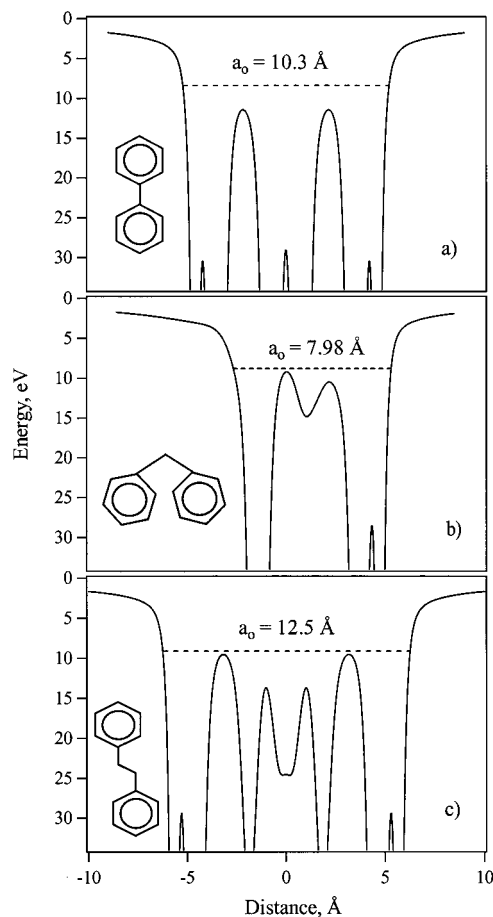


Figure 2. One-dimensional potential energy surfaces containing the characteristic lengths for (a) biphenyl, (b) diphenylmethane, and (c) diphenylethane. The dashed lines, illustrating the characteristic lengths of the molecules, are drawn at the level of the respective ionization potentials.

ionization potential of a molecule in the strong field, IP' , is expected to increase with the electric field strength, E , approximately by the value $U_p = (e^2 E^2 / 4m_e \omega_l^2)$,^{17,18} the ponderomotive potential of an electron under the influence of a radiation

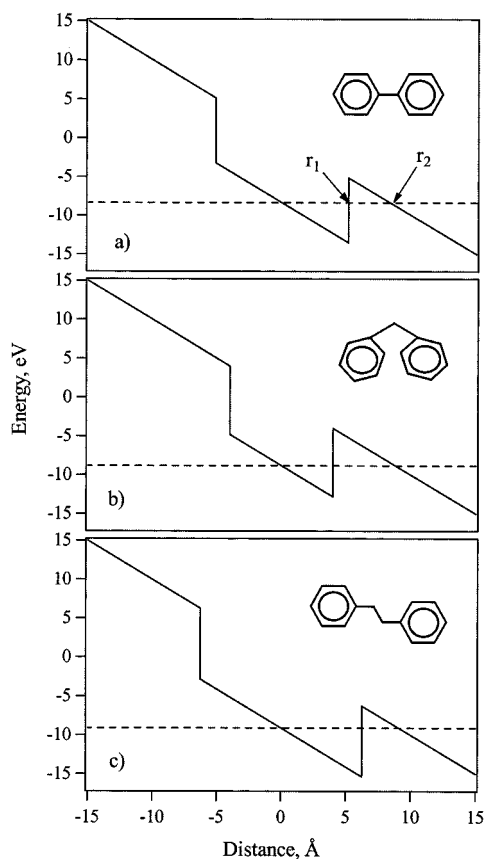


Figure 3. Potential energy surfaces shown in Figure 2 approximated by one-dimensional rectangular wells for (a) biphenyl, (b) diphenylmethane, and (c) diphenylethane. The width and the height of a well are given by the characteristic length and ionization potential, respectively.

field. Here e is the electron charge, m_e is the electron mass, and ω_1 is the laser frequency. As a first approximation, we assume that the ionization potential of these molecules in the strong field is increased by the value of the U_p . Using an 800 nm laser, U_p is 3.0 eV at $5 \times 10^{13} \text{ W} \cdot \text{cm}^{-2}$, representative of the IP shifts in the range of laser intensities used in this work. The effect of polarizability on molecular ionization potential has not been included in any theoretical treatment to date.

The increase in the ionization potential due to the ponderomotive potential results in a decrease in the tunnel ionization probability compared to that calculated for a molecule using the field free ionization potential. The increase in the ionization potential should also decrease the characteristic length, and this will result in a further reduction of the calculated ionization probability in comparison with that determined using the field free characteristic length. The effect of changing the characteristic length on the tunnel ionization rates is relatively insignificant in comparison with the effect of the field-induced changes in the ionization potential. Therefore, in these calculations we use field-induced ionization potential values of $\text{IP}' = \text{IP}_0 + U_p$, in conjunction with the field-free characteristic lengths of these systems.

The rectangular one-dimensional wells for each molecule with an electric field of $1.23 \text{ V} \cdot \text{\AA}^{-1}$ ($2 \times 10^{13} \text{ W} \cdot \text{cm}^{-2}$) superimposed are shown in Figure 3. Note that while the characteristic length of diphenylethane is larger than that of biphenyl, the smaller IP of biphenyl offsets this difference resulting in a similar barrier to tunnel ionization, and thus, the field ionization probabilities are expected to be similar for these two molecules. It is evident

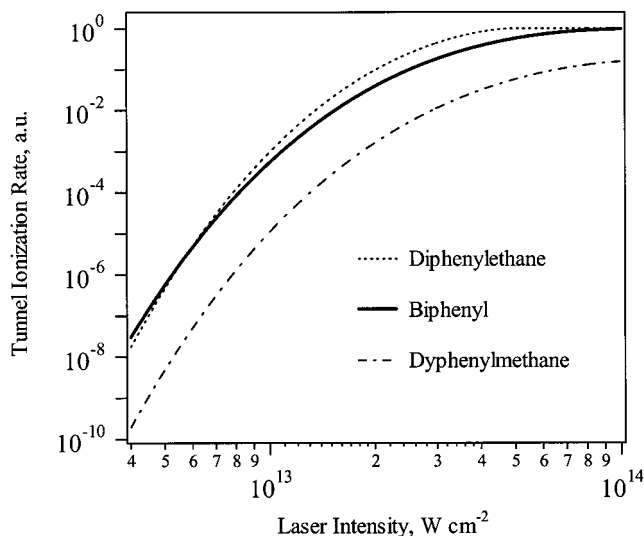


Figure 4. Tunnel ionization probability for biphenyl (solid line), diphenylethane (dash line), and diphenylmethane (dot-dash line) vs laser intensity. The calculation employs the field-free characteristic length and field-induced ionization potential, IP' , as described in the text.

that the barrier to tunnel ionization is larger in diphenylmethane in comparison with the other two molecules. Applying the Wentzel–Kramers–Brillouin (WKB) approximation, the probabilities for transmission of electronic wave packet through the barrier can be calculated using the equation

$$w = \exp\left\{-2 \int_{r_1}^{r_2} [2(\text{IP}' - V(r))]^{1/2} dr\right\} \quad (1)$$

where $V(r)$ is the perturbed potential barrier and r_1 and r_2 are the classical turning points determined by the ionization potential and the field-perturbed electrostatic potential energy surface.

The absolute tunnel rates for biphenyl, diphenylmethane, and diphenylethane, calculated using eq 1 as a function of laser intensity, are shown in Figure 4. The tunnel ionization probabilities for biphenyl and diphenylethane are similar and are both more than 1 order of magnitude higher than that for diphenylmethane. This suggests that as the laser intensity is increased, the diphenylethane and biphenyl are more likely to enter a regime where field ionization dominates other ionization mechanisms, in comparison to diphenylmethane.

The absence of discrete photoelectron peaks may be correlated to the lifetime of the neutral molecule in the intense laser field. If one assumes that an eigenstate will survive no longer than the time required to tunnel ionize, the tunnel ionization rates (in atomic units), w , arrived at using the WKB formalism may be considered as the inverse of the upper limit of eigenstate lifetime. The uncertainty in the lifetime is on the order of the inverse of the tunnel ionization rate, i.e., $\Delta t \sim w^{-1}$. Using the Heisenberg uncertainty principle, $\Delta E \Delta t \geq \hbar$, we see that $\Delta E \geq w$, in atomic units. Table 1 presents absolute transmission probabilities for the three molecules in question. The uncertainty in electronic eigenvalues ranges from $\sim 0.045 \text{ eV}$ for diphenylmethane to $\sim 2.66 \text{ eV}$ for diphenylethane at $1.23 \text{ V} \cdot \text{\AA}^{-1}$ ($2 \times 10^{13} \text{ W} \cdot \text{cm}^{-2}$). At this field strength, the uncertainty in electronic eigenvalue for biphenyl and diphenylethane is sufficiently large that a dramatic broadening of photoelectron peaks would be expected. If the ATI features are spaced by a value comparable to the broadening, a featureless distribution should result. The photoelectron distributions for biphenyl and diphenylethane show little evidence for discrete photoelectron peaks, in keeping

with the quantitative prediction of the lifetime broadening model. Diphenylmethane has a rather modest electronic eigenvalue uncertainty at similar field strengths, suggesting that the resolved ATI peaks of diphenylmethane would not smear into a continuum by the field-induced eigenstate broadening mechanism compared to the other two molecules.

Obviously, when ionization mechanisms other than tunnel ionization are considered, the molecules may ionize at intensities lower than the peak laser intensity. In the context of the lifetime broadening picture, this would tend to increase the resolution of the photoelectron peaks. However, the general trend of increased broadening with increased characteristic length is expected to remain valid.

We now consider whether the loss of discrete ATI photoelectron peaks in biphenyl and diphenylethane could be explained by incoherent emission of photoelectrons due to onset of NMED in these molecules. Any incoherent emission will destroy the interference effects leading to the ATI features in the photoelectron distributions. When polyatomic molecules are subjected to strong nonresonant fields, the lowest frequency electronic transitions may determine the field intensity for the onset of NMED, leading to rapid energy deposition in these molecules.² In the NMED model, one considers the amplitude of oscillation of an electron in oscillating electric field given by $a_{\text{osc}} = eE/m_e\omega_L$. If the amplitude of oscillation of the electron inside the potential energy surface is small compared to the characteristic length of the molecule, the electron dynamics may become highly nonadiabatic. The delocalized electrons will quiver inside the molecule with a typical energy on the order of U_p , the ponderomotive potential. Any scattering in the presence of the field, either from corrugation of the potential or from other electrons, will lead to the absorption/emission of energy U_p , similar to laser-assisted bremsstrahlung.¹⁹ When the U_p approaches the ionization potential or the characteristic electronic energy level spacing of the system, the excitation may become highly nonadiabatic.^{2,20} The probability for nonresonant Landau–Zener transition from one electronic surface to another scales as²

$$\exp(-\pi\Delta_0^2/4\omega_L EL) \quad (2)$$

where L is one-half of the characteristic length of a molecule. Ivanov and co-workers² have proposed that when $\omega_L EL \sim \Delta_0^2$ strong nonresonant absorption may occur leading to rapid energy deposition in the molecule.

The UV–visible absorption spectra for biphenyl, diphenylmethane, and diphenylethane reveal that the values of Δ_0 (defined here as the point where the molar absorptivity reaches 10^3) are 280, 230, and 225 nm, respectively. The values of Δ_0 for these molecules can be used to calculate the scaling factor for the Landau–Zener transition probability (eq 2) as a function of laser intensity at 800 nm, as shown in Figure 5. Biphenyl and diphenylethane have similar transition probabilities rising rapidly above $5.0 \times 10^{12} \text{ W}\cdot\text{cm}^{-2}$ and reaching saturation above $1.0 \times 10^{14} \text{ W}\cdot\text{cm}^{-2}$. Diphenylmethane has significantly reduced transition probability compared to these two molecules. The plot reveals that at all laser intensities the energy deposition by the NMED mechanism should increase in the series diphenylmethane \ll diphenylethane $<$ biphenyl. This is in qualitative agreement with all of the spectra shown in Figure 1. To understand whether rapid decoherence by the NMED mechanism is expected to play a major role in the energy deposition in any of these molecules at the field intensities employed, we calculate (using the criteria of $\omega_L EL \sim \Delta_0^2$) the laser intensities for the onset of NMED, I_{nmcd} , and list them in Table 1. The

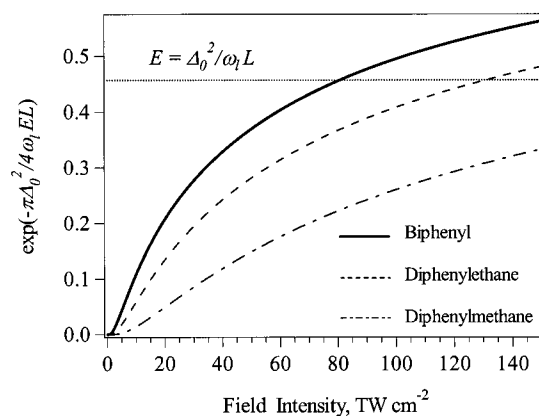


Figure 5. Scaling factor of the probability for nonresonant Landau–Zener transition for biphenyl (solid line), diphenylethane (dash line), and diphenylmethane (dot–dash line) vs laser intensity. The dotted line intercepts the probability curves at the field intensity of I_{nmcd} .

calculation predicts that the electron dynamics should remain adiabatic up to intensities of 8.0×10^{13} , 1.3×10^{14} , and 2.0×10^{15} for biphenyl, diphenylethane, and diphenylmethane, respectively. Therefore, we conclude that energy deposition by the NMED mechanism does not explain the loss of discrete ATI photoelectron peaks in biphenyl and diphenylethane. The threshold value for I_{nmcd} has been shown to be in agreement with the onset of extensive dissociation in recent experiments on anthracene, 9,10-dihydroanthracene and 1,2,3,4,5,6,7,8-octahydroanthracene.⁴

The influence of the field-induced state shifting on the ionization potentials and characteristic lengths, and consequently, on the tunnel ionization probabilities of these molecules has been discussed. It is also likely that the HOMO–LUMO energy gap does not remain constant in the strong dynamic fields employed in this work. Inclusion of the Δ_0 dependence on the laser field strength should increase the estimated intensity for the onset of NMED in these molecules. This is because the field-induced eigenstate shifting typically leads to increase in the separation of the energy levels in a system. Therefore, the I_{nmcd} values should be considered as the lower limits of the field intensities for the onset of NMED in these molecules.

Alternative mechanisms could be responsible for the broadening and washing out of the resolved features in photoelectron spectra presented here. For example, if the ionization proceeds via first populating excited states and then coupling these states to the continuum, one prerequisite for the observation of resolved peaks is that the excited states be locked at a fixed energy difference relative to the ionization threshold during ionization.²¹ Otherwise, the photoelectron signal from these states is expected to be smeared in energy space. It is possible that at sufficiently high laser intensities the excited states participating in the ionization undergo differential field-induced shifting relative to the ionization threshold. Another possibility is that as the laser intensity is increased, new ionization channels open, and the extra photoelectron signal overlaps in energy space with that corresponding to the low-energy channels, the latter are always present due to the temporal and spatial profile of the laser pulse. It is important to note that the loss of features in the photoelectron spectra presented here may not be unambiguously attributed to any one particular mechanism. We have shown that the electronic eigenstate lifetime broadening mechanism (in the context of the structure-based model) is sufficient to explain the results presented here.

The final observation we make from the photoelectron measurements of Figure 1 concerns the probability for electron

rescattering in these polyatomic molecules. In the studies of intense field ionization of atoms, the maximum kinetic energy of photoelectrons in the absence of electron rescattering is limited to twice the ponderomotive energy, $2 U_p$.²² For the electrons undergoing rescattering, the electron kinetic energies may range up to $8\text{--}10 U_p$.²³ Electron rescattering is known to be a rather ineffective process in the case of atomic tunnel ionization. In the tunnel ionization regime, an electron enters the continuum at a significant distance from the ion core (at the outer classical turning point of the electrostatic PES) and then undergoes oscillatory motion at the laser frequency ω_l . Immediately after being released from the atom in the ionization event, the electron wave packet undergoes a transverse delocalization. Numerical studies on intense-field ionization of helium have shown that the returning electron wave packet has a radius of approximately $30a_0$ as it rescatters from the nucleus.²⁴ Given the small dimensions of atoms, the transverse electronic wave packet delocalization result in low probability of recollision of the electron and the ion core. As a result, only a small fraction of photoelectrons (typically $\ll 1\%$) are detected with energies above $2 U_p$ in atomic tunnel ionization. In our case of strong-field ionization of polyatomic molecules, the values of the WKB transmission probability indicate that tunnel ionization should have a significant contribution to the detected electron signal, and therefore, we should expect electron rescattering to be active. In fact, we observe a significantly larger electron signal in excess of $2 U_p$ than is typical in atomic strong field ionization (the ponderomotive energies are 2.16, 2.88, 3.96, and 5.4 eV at the laser at intensities of 3.6, 4.8, 6.6, and $9.0 \times 10^{13} \text{ W}\cdot\text{cm}^{-2}$, respectively). This suggests that for the polyatomic molecules the electron rescattering may be more effective in comparison with atoms as suggested elsewhere.⁷ The dramatically increased spatial extent of these molecules (compared to atoms) enhances the probability for recollisions of the returning electrons with the ion core and should account for these measurements.

Conclusions

The strong-field photoelectron spectra are presented for biphenyl, diphenylmethane, and diphenylethane, a series of molecules containing two phenyl rings. The photoelectron spectra for biphenyl and diphenylethane are qualitatively similar, dominated by a broad, featureless distribution of electron kinetic energies over the range of laser intensities studied. Diphenylmethane displays discrete photoelectron peaks at the lower laser intensities investigated here but evolves to the featureless distribution as the laser intensity is increased. The number of atoms increases in the series biphenyl, diphenylmethane, and diphenylethane. The characteristic length, however, does not increase in this series but is considerably smaller for the diphenylmethane than for biphenyl or diphenylethane. The latter two molecules have similar characteristic lengths. The field ionization probability, therefore, is markedly different for diphenylmethane compared to the other two molecules. The loss

of discrete photoelectron peaks is consistent with a field-induced eigenstate lifetime broadening mechanism. According to this mechanism the lower tunnel ionization probability for diphenylmethane results in longer lifetimes of the electronic eigenstates populated during the excitation and consequently lower uncertainty in eigenstates' energy.

Acknowledgment. This work has been supported by the National Science Foundation (CHE-9976476). We also acknowledge the generous support of the Sloan and Dreyfus Foundations. We also thank Muhannad Zamari and Madhavan Narayanan for help with calculating the electrostatic potential energy surfaces.

References and Notes

- (1) Markevitch, A. N.; Moore, N. P.; Levis, R. J. *J. Chem. Phys.* **2001**, *267*, 131.
- (2) Lezium, M.; Blanchet, V.; Rayner, D. M.; Villeneuve, D. M.; Stolow, A.; Ivanov, M. Y. *Phys. Rev. Lett.* **2001**, *86*, 51.
- (3) DeWitt, M. J.; Levis, R. J. *Phys. Rev. Lett.* **1998**, *81*, 5101.
- (4) Markevitch, A. N.; Moore, N. P.; Levis, R. J. *Phys. Rev. A* **2001**, Submitted.
- (5) Agostini, P. F.; Fabre, F.; Mainfray, G.; Petite, G.; Rahman, N. K. *Phys. Rev. Lett.* **1979**, *42*, 1127.
- (6) DeWitt, M. J.; Levis, R. J. *J. Chem. Phys.* **1999**, *110*, 11368.
- (7) Moore, N. P.; Levis, R. J. *J. Chem. Phys.*, submitted.
- (8) Keldysh, L. V. *Sov. Phys. JETP* **1965**, *20*, 1307.
- (9) Ammosov, M. V. D.; N. B.; Krainov, V. P. *Sov. Phys. JETP* **1986**, *1191*.
- (10) Bardeen, C. J.; Yakovlev, V. V.; Wilson, K. R.; Carpenter, S. D.; Weber, P. M.; Warren, W. S. *J. Chem. Phys. Lett.* **1997**, *280*, 151.
- (11) Weinacht, T. C.; White, J. L.; Bucksbaum, P. H. *J. Phys. Chem. A* **1999**, *103*, 10166.
- (12) Assion, A.; Baumert, T.; Bergt, M.; Brixner, T.; Kiefer, B.; Seyfried, V.; Strehle, M.; Gerber, G. *Science* **1998**, *282*, 919.
- (13) Levis, R. J.; Menkir, G. M.; Rabitz, H. *Science* **2001**, *292*, 709.
- (14) Judson, R. S.; Rabitz, H. *Phys. Rev. Lett.* **1992**, *68*, 1500.
- (15) Levis, R. J.; DeWitt, M. J. *J. Phys. Chem. A* **1999**, *103*, 6493.
- (16) Frisch, M. J.; Trucks, G. W.; Schlegel, H. B.; Scuseria, G. E.; Robb, M. A.; Cheeseman, J. R.; Zakrzewski, V. G.; Montgomery, J. A., Jr.; Stratmann, R. E.; Burant, J. C.; Dapprich, S.; Millam, J. M.; Daniels, A. D.; Kudin, K. N.; Strain, M. C.; Farkas, O.; Tomasi, J.; Barone, V.; Mennucci, B.; Cossi, M.; Adamo, C.; Jaramillo, J.; Cammi, R.; Pomelli, C.; Ochterski, J.; Petersson, G. A.; Ayala, P. Y.; Morokuma, K.; Malick, D. K.; Rabuck, A. D.; Raghavachari, K.; Foresman, J. B.; Ortiz, J. V.; Cui, Q.; Baboul, A. G.; Clifford, S.; Cioslowski, J.; Stefanov, B. B.; Liu, G.; Liashenko, A.; Piskorz, P.; Komaromi, I.; Gomperts, R.; Martin, R. L.; Fox, D. J.; Keith, T.; Al-Laham, M. A.; Peng, C. Y.; Nanayakkara, A.; Challacombe, M.; Gill, P. M. W.; Johnson, B.; Chen, W.; Wong, M. W.; Andres, J. L.; Gonzalez, C.; Head-Gordon, M.; Replogle, E. S.; Pople, J. A. *Gaussian 99*, Development Version, revision B.08+; Gaussian, Inc.: Pittsburgh, PA, 2000.
- (17) Pan, L.; Armstrong, L., Jr.; Eberly, J. H. *J. Phys. B—At. Mol. Opt. Phys.* **1986**, *3*, 1319.
- (18) Freeman, R. R.; Bucksbaum, P. H. *J. Phys. B—At. Mol. Opt. Phys.* **1991**, *24*, 325.
- (19) Murnane, M. M.; Kapteyn, H. C.; Rosen, M. D.; Falcone, R. W. *Science* **1991**, *251*, 531.
- (20) Delone, N. B.; Krainov, N. B. *Atoms in Strong Laser Fields*; Springer-Verlag: Berlin, 1985.
- (21) DeBoer, M. P.; Muller, H. G. *Phys. Rev. Lett.* **1992**, *68*, 2747.
- (22) Corkum, P. B. *Phys. Rev. Lett.* **1993**, *71*, 1994.
- (23) Sheehy, B.; Lafon, R.; Widmer, M.; Walker, B.; DiMauro, L. F.; Agostini, P. A.; Kulander, K. C. *Phys. Rev. A* **1998**, *58*, 3942.
- (24) Walker, B.; Sheehy, B.; DiMauro, L. F.; Agostini, P.; Schafer, K. J.; Kulander, K. C. *Phys. Rev. Lett.* **1994**, *73*, 1227.